Optical trap setup for measuring microtubule pushing forces

J. W. J. Kerssemakers,[a] M. E. Janson, A. van der Horst, and M. Dogterom
F.O.M. Institute for Atomic and Molecular Physics, Kruislaan 407, 1098 SJ Amsterdam, The Netherlands

(Received 22 May 2003; accepted 30 September 2003)

We present an optical trap design for force measurements of polymerizing microtubules. These stiff, filamentous cell components contribute to dynamic processes by generating pushing forces, for example during cell division. Although single traps are widely used for molecular pulling processes, studying pushing by flexible filaments requires extra measures. We introduce multiple, asymmetric traps for directional stabilization and bracing of the microtubules for enhanced rigidity. Our method performs in a force range which was inaccessible so far, namely near the stall force of a polymerizing microtubule. The described methods open the way to the study of other polymerizing biomolecular systems as well. © *2003 American Institute of Physics.* [DOI: 10.1063/1.1629796]

Optical traps are a common tool to study piconewton forces generated by a wide range of biological systems, such as motor proteins, DNA polymerases, and unfolding proteins.[1] Typically, a laser with a continuous power of $\sim 10^2$ mW is focused tightly into a diffraction-limited spot of about 1 μm. In the focus, small particles can be trapped, provided their relative refractive index is sufficiently high.[2] Typical trap experiments involve biochemically prepared beads, linked to specific proteins or cell components. Small ($\sim 10^2$ nm) out-of-center displacements of a trapped bead cause a proportional restoring force, and thus a calibrated trap serves as a force sensor with stiffness k ($\sim 10^{-1}$ pN/nm).[3]

In general, optical tweezer experiments involve molecules that exert a pulling force on a trapped bead.[1,4] However, there are also biomolecular systems where pushing plays a central role. Examples are actin polymerization during *Listeria* propulsion[5] and nuclear positioning by microtubule polymerization in fission yeast cells.[6] In this letter, we present a special optical trap for measuring such pushing forces, in this work those of polymerizing microtubules. The setup is schematized in Fig. 1(a).

A microtubule (MT) consists of 8 nm long $\alpha\beta$-tubulin dimers, forming ~13 strands that polymerize into a hollow tube of approximately 25 nm diameter, see Fig. 1(b). The tube length ranges from a few up to $\sim 10^4$ dimers. In the living cell, apart from providing mechanical support as part of the cytoskeleton, MTs play an active role in dynamic structures such as the mitotic spindle.[7] At the basis of the active role of MTs lies *dynamic instability*:[8] under the influence of GTP hydrolysis, a single MT alternates repeatedly between states of prolonged growth (polymerization) and shrinkage, both in a cell (*in vivo*) and with purified tubulin outside a cell (*in vitro*).[9]

In vivo and *in vitro* experiments have confirmed that polymerizing MTs apply ~pN pushing forces,[10] large enough to play a role in cellular dynamics.[6,7] A decrease in growth velocity under increasing load was found *in vitro* by buckling experiments,[10] where MTs grow from nucleation sites against rigid barriers. Both the force and the growth rate are inferred from curvature analysis of the elastic MT. Eventually, growth should stop at the stall force. The magnitude of this stall force is an important input parameter for MT tip structure models.[11,12] However, the stall force can only be reached if the growing MT does not buckle before under the increasing load. This implies that inferring a stall force by buckling analysis is impossible. Further, the buckling method relies on a known rigidity of the MT. This parameter requires elaborate analysis to determine[13] and may vary considerably depending on the growth conditions.[14]

As an alternative we employed a multiple optical trap,[15] with a ''construct'' of two beads biochemically connected[16] to a MT segment, as in Fig. 1(a). One bead in a single trap would not suffice, as the pushing filament would tend to slide along the barrier. Buckling of the rather flexible segment between the two beads, as schematized in Fig. 2(a), is prevented by an asymmetric ''keyhole'' shaped trap potential, shown in Fig. 2(b): in a trapped construct, one bead is tightly trapped, while the other is only constrained in its sideways motion. As a result, the keyhole trap opposes pushing only with the bead closest to the barrier, and no buckling can occur between the two beads. We realized this keyhole trap with a single laser, time-shared between different spatial positions by means of software-driven acousto-optical deflec-

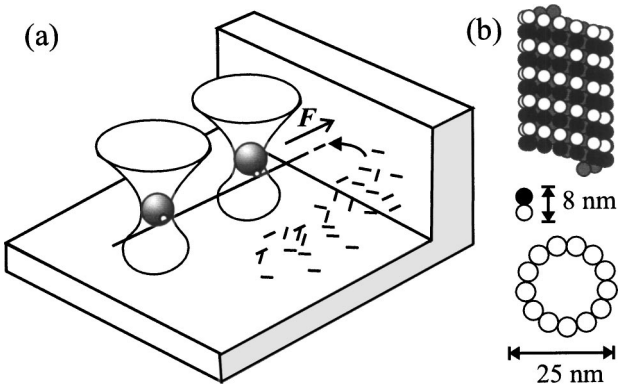

FIG. 1. (a) Schematics of a biomolecular pushing experiment, where a growing (polymerizing) filament is trapped in front of a rigid barrier. Elongation of the filament pushes the connected beads backward in the traps, from which the pushing force F is inferred. The second trap is necessary for stabilization of the pushing direction. (b) Structure of a microtubule. During polymerization, new tubulin dimers add to the end forming a helical tube.

[a]Electronic mail: j.kerssemakers@amolf.nl

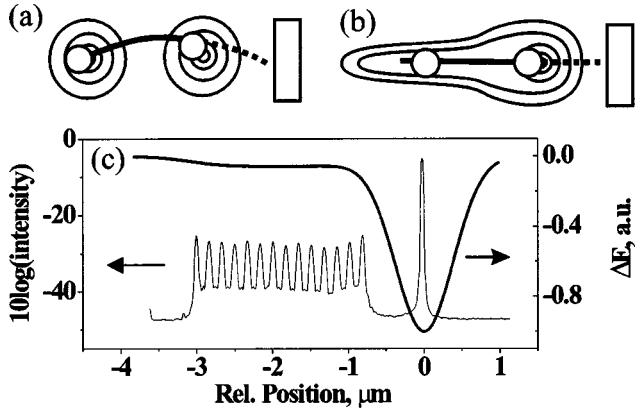

FIG. 2. Optimizing the pushing configuration. (a) A growing flexible filament suspended in a double trap tends to buckle, which can be prevented by making an asymmetric trap as shown in (b): fast time sharing of the laser beam is used to trap one bead tightly, while the other bead is only trapped perpendicular to the pushing direction. In this geometry, only the growing end of the microtubule may buckle. The trap potential is constructed as shown in (c). Thin line: power spectrum of laser deflector input. The amplitude is a measure for occupation time vs position of the laser beam. Thick line: effective trapping potential, approximated by weighted summation of single laser potentials.

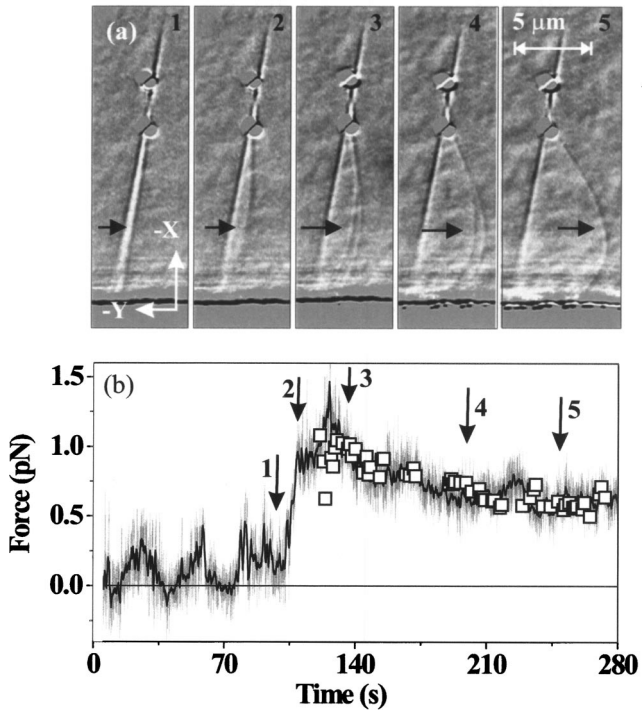

FIG. 3. (a) Sequence of differential microscopy images of two growing and pushing microtubules (arrows), suspended via two beads in a keyhole trap. Increased buckling is visible as the microtubules grow (the left static microtubule is an artifact from the image enhancement). (b) Continuous curve: time sequence of the force on the lower bead in the x direction (gray) and a running average (black, 2 s average). Open squares: force derived from curve analysis of the buckling microtubules. Both measurements reflect the same qualitative behavior, typical for a touch-and-buckle event.

tors. The frequency of the deflector input signal determines the laser spot position. Therefore, a power spectrum [Fig. 2(c), thin line] of this input signal indicates also the relative occupancy time of the laser for the various positions. At high enough time-sharing frequency, a bead will experience an effective, time-averaged potential from the trap, approximated by appropriately summing single laser potentials [Fig. 2(c), thick line].[15]

A second measure we introduce to prevent buckling is to stiffen the construct itself, as is shown later on. Then, only the ''free'' growing end of a MT can contribute significantly to buckling.

We compared the trap approach with the established buckling analysis in a pilot experiment shown in Fig. 3(a). From a trapped construct, two MTs were growing long enough to buckle against a barrier long before stalling would occur. Differential microscope images show the increasing buckling of both MTs (the left straight microtubule is an image enhancement artifact). We used the microscope images to infer the pushing forces in two ways. First, motion tracking of the lower bead provides us both with a bead displacement vs. time and, via the trap stiffness,[15] with a force [Fig. 3(b), gray: raw signal; black line: 2 s running average]. Apart from the thermal motion of the bead, we see that around $t=105$ s the force steeply rises, indicating a pushing event. In accordance with a buckling sequence, the pushing force reaches a maximum (here 1.2 ± 0.2 pN) after which it drops.

Second, curve analysis[10] was used to estimate the total force acting on the MT tips together. The shapes of both MTs were curve fitted separately and the inferred forces were summed. The data of the buckling analysis [open squares in Fig. 3(b)] coincides well with those of the trap measurements if we assume a MT bending rigidity κ of $\sim 6.7\ \mathrm{pN}\,\mu\mathrm{m}^2$, a value at the low end of reported values.[13,14] Note that before and at the onset of pushing, the absence of buckling inhibits data acquisition (before image 3). Thus, for the range where both methods are applicable, we find the same qualitative behavior.

As noted before, stall forces cannot be measured with buckling analysis. With the trap, they can be, as we show in a next pilot experiment (Fig. 4). Here, no keyhole trap was used, but instead a bundle of ~20 cross-linked MTs was used for the construct. The enhanced rigidity of this bundle prevents buckling of the segment between the two beads. The preparation method of these bundles causes only a few of these MTs to nucleate.[16] As shown in Fig. 4(a), the bundle was kept at $\sim 5\ \mu$m from a barrier, in this case a large, corrugated silica bead attached to the substrate. The short distance of the free growing MTs to the barrier excludes buckling of these ends.

In this particular experiment, only the left bead in Fig. 4(a) was tightly connected to the bundle, which implies that the total pushing force could be inferred from the displacement of this bead only, as shown in Fig. 4(b). In the first curve, we observe two persistent increases in force, followed by distinct plateaus. We interpret this as an event where the first one growing MT touches the wall, followed by a second MT joining in at $t\sim 650$ s.[17] From there, we measure two *synchronized* MTs. After full retraction of the whole construct, the force returns to zero after which a second contact event is observed.

The white squares in Fig. 4(b) indicate binned averages (over 8 s intervals), which were subsequently used to yield a pilot force-velocity curve, Fig. 4(c). The data converge to two stall forces at ~1.2 and ~3 pN for the single- and double-MT case, respectively. The low initial velocities of

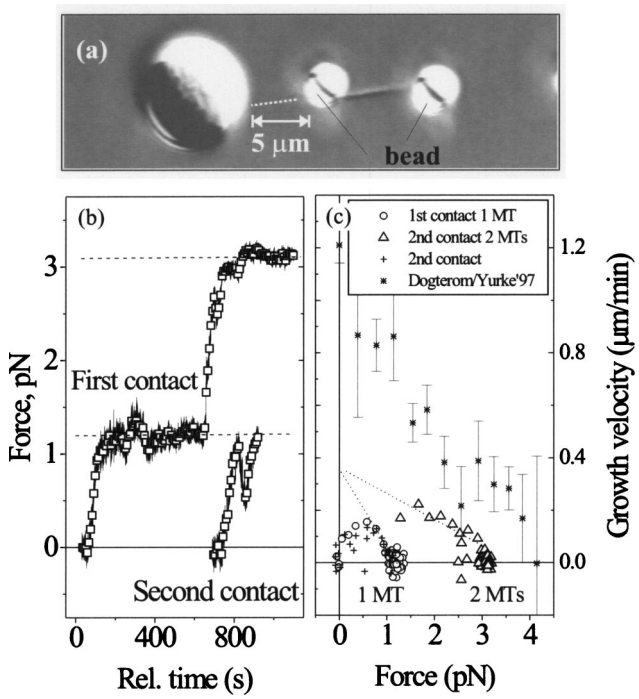

FIG. 4. (a) Stall force measurements on growing microtubules nucleated by a MT bundle, held by two trapped beads in front of a substrate-fixed barrier (a large, corrugated bead). The growing end (invisible) is indicated by the dotted line. (b) Force on the left trapped bead. The two plateaus suggest that two microtubules touch and push one after another against the wall. After full retraction, a second growth event is observed (right curve). The white squares indicate binned averages over 8 s. (c) Averaged force vs growth velocity, inferred from (b). The data discriminate between one (down triangles and diamonds) and two (up triangles) microtubules against the wall. The more accurate high-force data suggest a common origin at zero-force (guide lines). Open circles show force data obtained with the buckling analysis at higher initial growth velocities (see Ref. 10).

the trap measurements are an experimental artifact, presumably caused by possible ''settling'' of the MT on the barrier or some deformation of the construct itself. We expect that for shorter free growing ends, or in a trap with lower stiffness, also the low-force range will give an accurate view of the growth velocity.

The stall force is expected to be proportional to the number of microtubules pushing.[18] Then, the high-force tails for the single and the double MT are expected to originate from one single point on the zero force axis, which is indeed suggested by the data (guide lines in the plot). As a comparison, results from buckling experiments performed at higher initial growth velocities are also plotted.[10] Again, such buckling analysis can only yield estimates of a stall force, which ends up somewhat higher than those directly measured with the trap. The difference is presumed to originate from the different initial, unloaded growth velocities in these experiments (1.2 and ~0.4 μm/min, respectively).

In conclusion, we have measured stall forces of pushing microtubules with an optical trap. This proof of principle experiment also opens the way to study microtubule growth dynamics with much larger spatial and temporal resolution than previously possible, as a trap in principle allows for high-frequency data acquisition.[3]

The trap method is complementary to the buckling analysis method: the latter more naturally applies to large length increases at low forces, while the trap measures stall forces on short length and time scales. In addition, the trap allows for ''force clamp'' techniques. From the present work it appears that for such studies, a rigid and stable construct is crucial. The two methods we introduced, an asymmetric ''keyhole'' trap and ''bracing'' of cross-linked filaments, may also allow to study force generation of much less rigid polymers such as single actin filaments.[5]

The authors thank T. Surrey and F. Nédélec for the kinesin plasmid and H. Bakker, S. Tans, and S. Woutersen for critical reading of the manuscript. This work is part of the research program of the ''Stichting voor Fundamenteel Onderzoek der Materie (FOM),'' which is financially supported by the ''Nederlandse Organisatie voor Wetenschappelijk Onderzoek (NWO).''

[1] A. D. Mehta, M. Rief, J. A. Spudich, D. A. Smith, and R. M. Simmons, Science **283**, 1689 (1999).
[2] A. Ashkin, Proc. Natl. Acad. Sci. U.S.A. **94**, 4853 (1997).
[3] K. Visscher, S. P. Gross, and S. M. Block, IEEE J. Sel. Top. Quantum Electron. **2**, 1066 (1996).
[4] T. Roopa and G. V. Shivashankar, Appl. Phys. Lett. **82**, 1631 (2003).
[5] L. A. Cameron, P. A. Giardini, F. S. Soo, and J. A. Theriot, Nature Reviews Molecular Cell Biology **1**, 110 (2000).
[6] P. T. Tran, L. Marsh, V. Doye, S. Inoue, and F. Chang, J. Cell Biol. **153**, 397 (2001).
[7] S. Inoue and E. D. Salmon, Mol. Biol. Cell **6**, 1619 (1995).
[8] A. Desai and T. J. Mitchison, Annu. Rev. Cell Dev. Biol. **13**, 83 (1997).
[9] D. K. Fygenson, E. Braun, and A. Libchaber, Phys. Rev. E **50**, 1579 (1994).
[10] M. Dogterom and B. Yurke, Science **278**, 856 (1997).
[11] A. Mogilner and G. Oster, Eur. Biophys. J. **28**, 235 (1999).
[12] M. Dogterom, M. E. Janson, C. Faivre-Moskalenko, A. Van der Horst, J. W. J. Kerssemakers, C. Tanase, and B. M. Mulder, Appl. Phys. A: Mater. Sci. Process. **A75**, 331 (2002).
[13] F. Gittes, B. Mickey, J. Nettleton, and J. Howard, J. Cell Biol. **120**, 923 (1993).
[14] M. E. Janson, Ph.D. thesis, Leiden University, The Netherlands, 2002.
[15] We trap with a Nd YVO_4 1064 nm laser (Spectra Physics). The trapped bead motion is detected with a He–Ne 633 nm laser and a quadrant photodiode for calibration purposes. We infer the stiffness from the roll-off frequency in the bead motion spectrum. The trap potential was measured by capturing beads in viscous glycerol, yielding a near-Gaussian profile with a width of app. 0.8 μm.
[16] We grow MTs in vitro from tubulin (Cytoskeleton Inc.) and GTP in MRB80 buffer (80 mM Pipes, 1 mM EGTA, 4 mM $MgCl_2$, PH 6.8) from GMPCPP-stabilized seed MTs or bundles (MTs clustered with avidin). Streptavidin beads are either connected to biotynilated MTs or attached via biotynilated, immobilized AMP–PNP–kinesin as an intermediate linker. The barriers are either predeposited SiO_x walls or silica porous beads (Asahi Glass Comp.).
[17] Parallel experiments (Janson, Ph.D. thesis) predict a catastrophe within ~30 s from the onset of stalling. The extended lifetime in this particular experiment is attributed to residual stabilizing agents in the growth solution.
[18] G. S. v. Doorn, C. Tănase, B. M. Mulder, and M. Dogterom, Eur. Biophys. J. **29**, 2 (2000).